American Mineralogist, Volume 83, pages 794–798, 1998

A convenient method for measuring ferric iron in magnesiowüstite ($MgO\text{-}Fe_{1-x}O$)

David P. Dobson,[1,*] Neil S. Cohen,[2] Quentin A. Pankhurst,[2] and John P. Brodholt[1]

[1] Department of Geological Sciences, University College London, Gower Street, London WCE6BT, U.K.
[2] Department of Physics and Astronomy, University College London, Gower Street, London WCE6BT, U.K.

Abstract

We present a new oxybarometer for magnesiowüstite-bearing systems, which is easily applied using widely available techniques. A scale relating the proportion of Fe^{3+} [$\alpha = Fe^{3+}/(Fe^{3+} + Fe^{2+})$] to the position of the (220) reflection and total Fe (y) in magnesiowüstites $(Mg_{1-y}\cdot Fe_y)_{1-x}O$ has been derived from measured values in samples equilibrated at various oxygen fugacities:

$$\alpha = 13.0047 - 39.4829f + 40.0540f^2 - 13.5701f^3(\pm 0.007 + 0.09\alpha),$$

$$f = (d_{220} - 1.4890)/(0.0510y + 0.0206y^2)(\pm 0.0001).$$

Previously established partition coefficients can then be used to relate estimated Fe^{3+} content to equilibrium oxygen fugacity (f_{O_2}) in the composition range $0 < y < 0.2$. Equilibrium oxygen fugacities of $\log f_{O_2} \leq -1.7$ can be estimated to ± 0.5 log units using just X-ray powder diffraction and electron microprobe analytical techniques.

Introduction

Accurate characterization of the equilibrium oxygen environment is fundamental to understanding the petrogenesis of many rocks. High-pressure experiments, however, commonly have poor control of the oxygen environment, which leads to uncertainties in the application of those results to natural systems. Although Mössbauer spectroscopy has proven extremely successful in measuring Fe^{3+} contents of non-stoichiometric minerals, this technique normally requires large sample volumes or synthetic samples enriched in the Mössbauer isotope ^{57}Fe. It would be convenient, therefore, to have a simple analytical technique to estimate the equilibrium oxygen fugacity of experimental and natural samples as an oxybarometer.

The wüstite family of oxides accommodates significant non-stoichiometry, and the solid-solution phase magnesiowüstite is present in some natural and synthetic assemblages. Magnesiowüstite is formed in the shallow crust by contact metamorphism of limestones or during emplacement and eruption of carbonatites. Additionally, magnesiowüstite is thought to be a major constituent of the lower mantle. Magnesiowüstite inclusions found in diamonds, which are thought to have originated in the lower mantle, were analyzed for Fe^{3+} by micro-Mössbauer spectroscopy (McCammon et al. 1995). Dobson et al. (1997) and Wood and Nell (1991) demonstrated that Fe^{3+} greatly affects the electrical conductivity of magnesiowüstite at the elevated T of the lower mantle. Biggar (1974) demonstrated that non-stoichiometry in magnesiowüstite causes significant lattice relaxation and suggested that the systematic variation of cell parameter with oxygen fugacity can be used as a standard for calibrating gas-mixing furnaces. The defect-structure and redox equilibria of magnesiowüstite were studied extensively (Brynstead and Flood 1958; Speidel 1967; Valet et al. 1975; Gourdin et al. 1979) and the formulation of Valet et al. (1975) accurately predicts the $T\text{-}P_{O_2}\text{-}$[Fe/(Fe+Mg)] dependence of Fe^{3+} content. We have used the data of Biggar (1974) along with new experimental data from the present study to quantify the dependence of cell parameter on Fe^{3+} in magnesiowüstite. We find that this produces an oxybarometer accurate to ± 0.5 log units at values of oxygen fugacity relevant to the Earth.

Experimental and analytical methods

Polycrystalline magnesiowüstite samples of 4.6, 10.0, 14.9, and 20.0 ± 0.1 mol% wüstite were synthesized by sintering stoichiometric mixtures of MgO, Fe_2O_3, and Fe at 1100 °C. After three to five 15 h cycles of grinding and sintering under the C-CO oxygen buffer, starting samples were homogeneous with Fe^{3+} below the detection limit by Mössbauer spectroscopy. Small aliquots (0.1 g) of these samples were then suspended on platinum wires and equilibrated with $CO\text{-}CO_2$ mixtures at 1 atm total P and 1300 °C for 4 h before quenching by withdrawing the wire to the top of the gas-mixing furnace. Quench rates thus obtained, of up to 400 °C/min, allowed monophase samples with up to 33% $Fe^{3+}/(Fe^{3+} + Fe^{2+})$ to be synthesized. To obtain higher Fe^{3+}/Fe, samples were synthesized in a Walker-type multi-anvil press at 50 kbar and 1300 °C. A 14 mm edge length octahedron of Aremco 584 castable ceramic was compressed using 8 mm truncation edge length WC anvils. Pressure was calibrated at room temperature using the transitions of Bi (2.5,7.7

* E-mail:d.dobson@ucl.ac.uk

0003–004X/98/0708–0794$05.00

GPa), Ba (5.5 GPa), and Sn (9.4 GPa) and, at 1100 and 1500 °C, using the phase changes fayalite-spinel and coesite-stishovite. The graphite furnace buffered the sample [the graphite-CO buffer is highly oxidizing under these conditions; at 50 kbar and 1300 °C, log $f_{O_2} = -5.5$ (Taylor and Green 1988)]. Samples were held at this T and P for 1 h after which power was cut to the furnace. This produced thermal quench rates of up to 1000 °C per second. The high quench rates combined with the increased stability field of magnesiowüstite at high pressure allowed reproducible synthesis of samples with 70% or more Fe^{3+}.

The oxidized samples were examined optically and analyzed by electron microprobe methods to evaluate chemical homogeneity. Cell parameters were measured on a Philips 2-circle powder diffractometer (Cu$K\alpha$ at 35 kV; 30 mA) with a quartz internal standard. Samples giving spectra with unattributable diffraction peaks were discarded (precision at 60° 2θ was 0.00015 Å). Samples were then analyzed by Mössbauer spectroscopy, using a constant acceleration unit in transmission geometry with an unpolarized 50 mCi source of ^{57}Co in Rh. Spectra were collected in 576 channels and folded to remove baseline curvature. The spectra were fitted using a least-squares method to Lorentzian sextets or doublets for magnetic and paramagnetic phases. Peak assignment was governed largely by the requirement that both the Fe^{3+} and Fe^{2+} doublets be symmetric, and that the Fe^{2+} sites have a self-consistent isomer shift of order 1.0 mm/s. Fe^{3+} contents measured by Mössbauer spectroscopy and those predicted from Valet et al. (1975) were within 2% for samples equilibrated with gas mixtures, consistent with the recoil-free fraction in the Fe^{3+} and Fe^{2+} sites being equal for magnesiowüstites. Samples that had disproportionated during quenching were easily identifiable by the characteristic sextet spectrum from the magnetic magnesioferrite phase (Fig. 1), within a detection limit on the order of 5 at%, and by the bright red color of the magnesioferrite.

Measurements reported by Biggar (1974) of d_{220} for magnesiowüstite samples equilibrated at 1065 °C and various oxygen fugacities have been incorporated using the equilibrium constants derived by Valet et al. (1975). This provides an independent test for the effect of varying quench T and preparation techniques on measured cell parameter. Results are presented in Table 1.

Results and discussion

For the purpose of modeling cell parameters in magnesiowüstite, it is convenient to consider initially the nominally stoichiometric binary MgO-FeO, which is extremely well modeled in the 0–20% wüstite region by a quadratic least-squares fit. Thus d_{220} in samples with $\alpha = 0$ in Table 1 [$\alpha = n_{Fe^{3+}}/(n_{Fe^{2+}} + n_{Fe^{3+}})$] can be modeled against wüstite concentration by:

$$d_{220}(\alpha = 0) = 1.4890 + 0.0510y + 0.0206y^2 \quad (1)$$

where d_{220} is the length (in angstroms) of the (220) reflector in the stoichiometric magnesiowüstite cell and $y = n_{Fe}/(n_{Fe} + n_{Mg})$. The uncertainity associated with Equation 1 is ±0.0001.

The effect of Fe^{3+} from oxidation of the wüstite component:

$$Mg^{2+} + 2Fe^{2+} + \tfrac{1}{2}O_2 = 2Fe^{3+} + MgO \quad (2)$$

is to reduce the unit-cell volume. This can be understood by considering the incorporation mechanism of Fe^{3+}, which can be contained in pure wüstite on interstitial or cation sites, charge balanced by vacancies (e.g., Hazen and Jeanloz 1984; Long and Grandjean 1991). In dilute solutions of wüstite, such as those under study here, interstitial Fe^{3+} is rare (Gourdin et al. 1979; Valet et al. 1975) and Fe^{3+} and vacancies exist on the NaCl structure cation sites. Incorporation of wüstite into periclase significantly increases the solubility of Fe^{3+} at high temperature, with values of $0.02 < Fe^{3+}/Fe < 0.7$ for 20% wüstite, without disproportionation (Hazen and Jeanloz 1984; Valet et al. 1975; Speidel 1967). For $0 < y < 0.2$ at T between $1300 < T\ °C < 1500$, Valet et al. (1975) suggested the reaction:

$$2Fe^{2+}_{Mg} + \tfrac{1}{2}O_2 = (Fe^{3+}_{Mg}\square Fe^{3+}_{Mg}) + O^{2-}_{O} \quad (3)$$

which conserves lattice sites and provides local charge balancing. The subscript denotes the lattice site and ($Fe^{3+}_{Mg}\square Fe^{3+}_{Mg}$) represents a charge-balanced dimer with two Fe^{3+} separated by a single cation vacancy. The net result is that these vacancies reduce the unit-cell volume.

We can define a function (f) for non-stoichiometric magnesiowüstite as follows: $f = (d_{220} - 1.4890)/[d_{220}(\alpha = 0) - 1.4890]$, which is a measure of the reduction in partial molar volume of the wüstite component due to Fe^{3+}, as found from X-ray diffraction experiments (see previous paragraph). A least-squares regression of α, measured by Mössbauer spectroscopy, on the function (Fig. 2), yields the equation:

$$\alpha = 13.0047 - 39.4829f + 40.0540f^2 - 13.5701f^3 \quad (4)$$

The uncertainty associated with Equation 4 is $\pm 0.007 + 0.09\alpha$. Thus Equation 4, together with Equation 1 can be used to estimate Fe^{3+} from measurements of d_{220} and Fe content.

Figure 3A shows the Mg-rich corner of the ternary system MgO-FeO-Fe_2O_3 with contours of equal volume, derived from Equations 1 and 4, and experimental data. The form of the dependence of α on f causes the d_{220} contours to become sub-parallel to the FeO-Fe_2O_3 sideline at high α, i.e., at high Fe^{3+} d_{220} becomes insensitive to Fe^{3+}. This causes an increase in uncertainty at high α (the uncertainty in α is approximately 10% relative between $0.15 < \alpha < 0.6$), but such oxidized samples are rare in nature. The reduction in sensitivity of d_{220} at high Fe^{3+} may be due to the formation of larger Fe^{3+} clusters that are stable with increasing Fe^{3+} at low temperature. These large clusters would have a smaller net effect on the cell parameter than more evenly dispersed cation vacancies. Alternatively, quenching highly oxidized magnesiowüs-

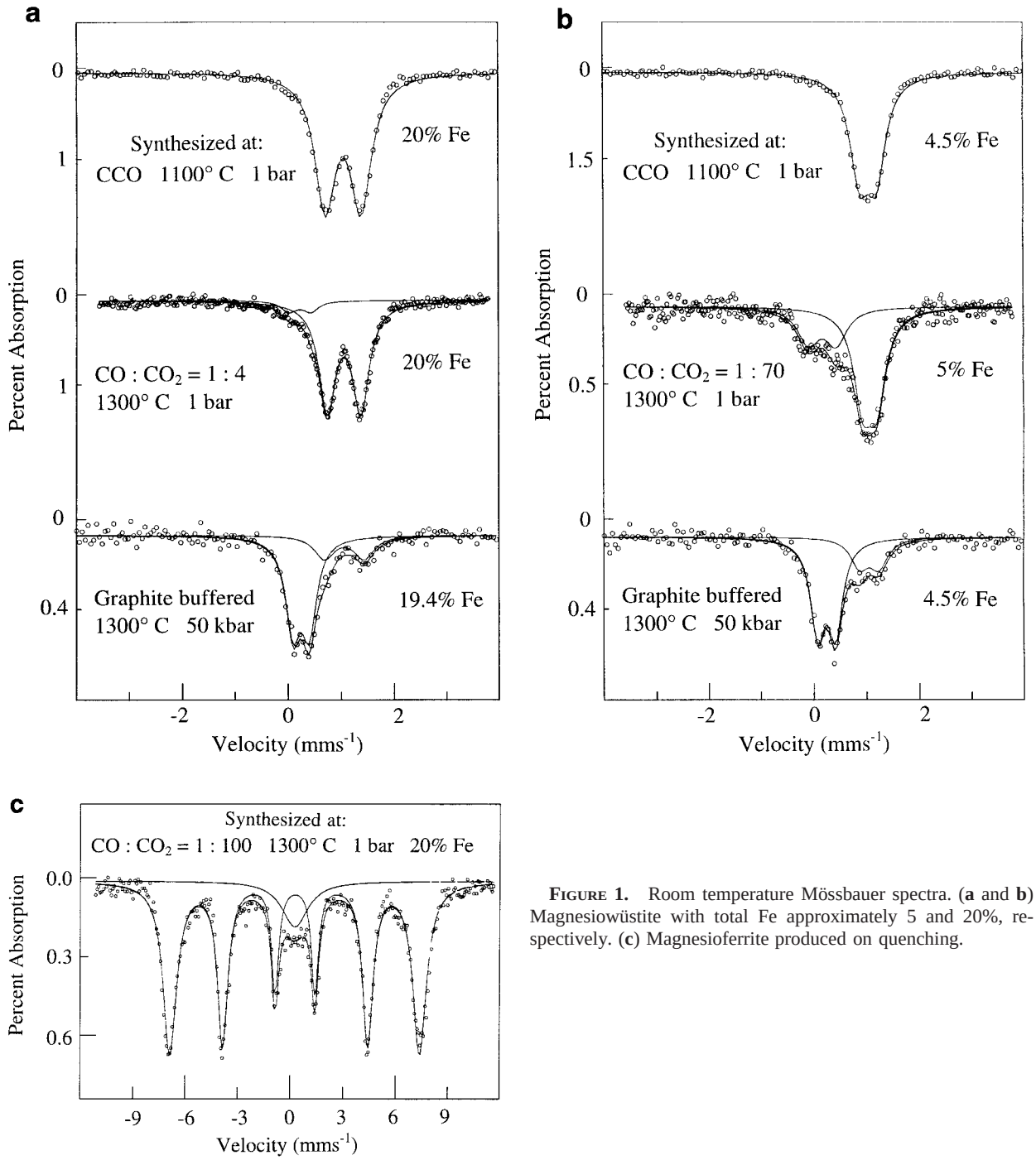

FIGURE 1. Room temperature Mössbauer spectra. (**a** and **b**) Magnesiowüstite with total Fe approximately 5 and 20%, respectively. (**c**) Magnesioferrite produced on quenching.

tites into the metastable region may produce quench spinel at an atomic level, as has been observed with magnetite in wüstite. Small amounts of sub-micrometer-sized magnesioferrite would not be detectable by the analytical methods employed here, requiring transmission electron microscopy. The close agreement, however, between predicted and measured Fe^{3+} contents imply that Fe^{3+} loss to quench phases is minimal.

OXYBAROMETRY

Now that we have a simple method for estimating Fe^{3+}, we can use the equilibrium constant for the incorporation of ($Fe^{3+}\square Fe^{3+}$) dimers (Eq. 3):

$$K = [(Fe^{3+}_{Mg}\square Fe^{3+}_{Mg})][O^{2-}_{O}]/([Fe^{2+}_{Mg}]^2 P^{1/2}_{O_2}) \quad (5)$$

where square brackets denote site occupancy. From charge- and mass-balance considerations we have:

TABLE 1. Fe^{3+} and Fe^{2+} determined by room temperature Mössbauer spectroscopy: isomer shift relative to α-iron (δ) and quadropole splitting (Δ), and d_{220} in magnesiowustite

$y = n_{Fe}/n_{Fe} + n_{Mg}$	Fe^{2+} δ (mm/s)	Fe^{2+} Δ (mm/s)	Fe^{3+} δ (mm/s)	Fe^{3+} Δ (mm/s)	$\alpha = n_{Fe^{3+}}/n_{Fe}$	d_{220} (Å)	$f(d_{220},y)$	log f_{O_2}	Notes
0.200	1.05(1)	0.68(1)	—	—	0.000	1.5000	0.9978	−11.40	*
0.200	1.04(1)	0.66(1)	0.25(1)	0.41(2)	0.022(2)	1.4995	0.9525	−10.07	†
0.200	1.05(1)	0.65(1)	0.28(3)	0.29(4)	0.065(9)	1.4985	0.8618	−9.75	†
0.200	1.05(1)	0.64(1)	0.28(2)	0.36(3)	0.077(8)	1.4981	0.8255	−8.50	†
0.200	1.06(1)	0.64(1)	0.23(2)	0.41(3)	0.088(8)	1.4972	0.7438	−7.49	†
0.200	1.05(1)	0.63(1)	0.10(1)	0.48(2)	0.233(11)	1.4970	0.7257	−6.59	†
0.194	1.06(3)	0.75(5)	0.24(1)	0.30(1)	0.738(31)	1.4960	0.6561	−5.5	‡
0.045	1.04(1)	0.31(1)	—	—	0	1.4913	0.9843	−11.40	*
0.050	1.06(1)	0.26(1)	0.17(1)	0.53(2)	0.331(13)	1.4908	0.6919	−6.01	†
0.045	1.05(2)	0.37(3)	0.24(1)	0.34(1)	0.721(25)	1.4904	0.5991	−5.5	‡
0.2	no Mössbauer data available				0.012	1.4994	0.9434	−11.60	§
0.2					0.026	1.4992	0.9253	−11.30	§
0.2					0.081	1.4982	0.8345	−10.20	§
0.2					0.097	1.4976	0.7801	−10.00	§
0.149					0	1.4970	0.9930	−11.40	*
0.100					0	1.4943	0.9989	−11.40	*
0.1					0.103	1.4934	0.8292	−9.35	§
0.000					—	1.4890	—	—	#

* Present study, equilibrated at C-CO, 1100 °C.
† Present study, gas mixing, 1300 °C.
‡ Present study, 50 kbar, C-CO, 1300 °C.
§ Biggar (1974), 1065 °C, error in Fe^{3+} unknown.
# JCPDS file 4-829.

$$2[(Fe^{3+}_{Mg}\Box Fe^{3+}_{Mg})] = [Fe^{3+}] = n_{Fe^{3+}}/(n_{Fe^{2+}} + n_{Fe^{3+}} + n_{Mg} + n\Box) = 2\alpha/(2 + 2A + \alpha), \quad (6)$$

and

$$[Fe^{2+}_{Mg}] = n_{Fe^{2+}}/(n_{Fe^{2+}} + n_{Fe^{3+}} + n_{Mg} + n\Box) = 2(1 - \alpha)/(2 + 2A + \alpha) \quad (7)$$

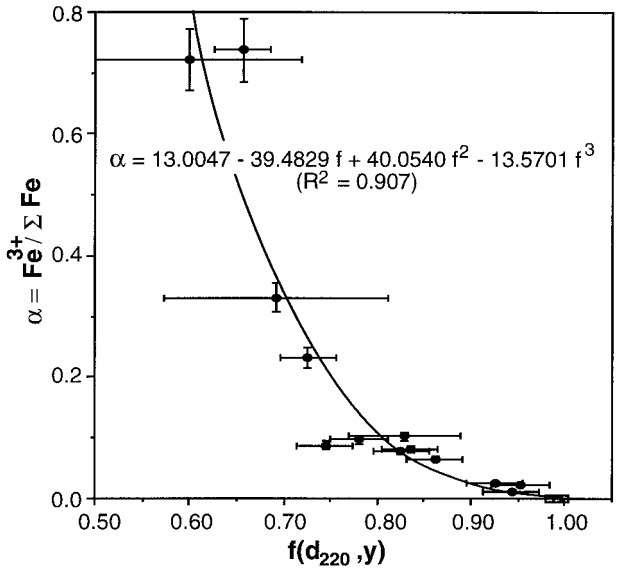

FIGURE 2. The effect of non-stoichimoetry on d_{220}: $f_{obs} = (d_{220(\alpha)} - 1.498)/(d_{220(0)} - 1.498)$. Solid circles are for samples equilibrated at various oxygen fugacities; open squares for nominally stoichiometric magnesiowüstite equilibrated at C-CO.

where $A = n_{Mg^{2+}}/(n_{Fe^{2+}} + n_{Fe^{3+}}) = (1 - y)/y$ and $[O^{2-}_{O}] = 1$.

Combining Equations 5 to 7 gives the equilibrium constant derived by Valet et al. (1975):

$$(P_{O_2})^{1/2} K = \alpha(2 + 2A + \alpha)/(1-\alpha)^2 \quad (8)$$

and

$$\log_{10}(K) = \frac{10754}{T} - 2.951 \quad (9)$$

for Equation 3; T is absolute temperature. K assumes all Fe^{3+} is incorporated as dimers, and reproduces thermogravimetric measurements for all $0 < \alpha < 0.75$ and $0 < y < 0.2$. Additionally, the close agreement between measured and predicted Fe^{3+} in our gas-mixing experiments confirms the accuracy of K across $0 < \alpha < 0.33$. At higher concentrations of Fe, however, Fe^{3+} dimers begin to interact, introducing a compositional dependence to the equilibrium constant. This interaction would also change the nature of the dependence of d_{220} on Fe^{3+} for values of $y > 0.2$. Figure 3B shows the dependence of d_{220} and α on cation composition and P_{O_2}.

This procedure estimates the oxygen fugacity for samples equilibrated at 1 atm total P. For Equations 1 and 4 to be applied to high-pressure samples, it must be assumed: (1) that the quenched-in Fe^{3+} content is the same as that at P; and (2) that the mechanism for incorporation of Fe^{3+} is the same as at low pressure. Additionally, for oxybarometry, the P dependence must be known for reaction 2. Accurate calibration of the P dependence of Fe^{3+} content is beyond the scope of the present study, although initial experiments at 50 and 100 kbar suggest, assuming 1 and 2 to be true, that the pressure dependence

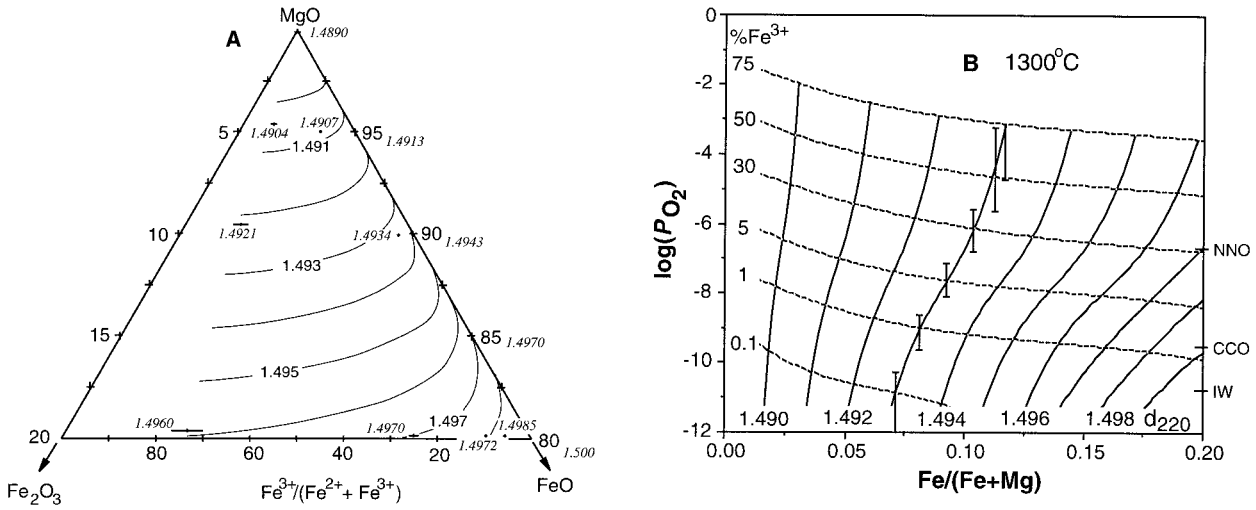

FIGURE 3. (**A**) Predicted d_{220} (solid lines) on MgO-rich portion of the MgO-FeO-Fe_2O_3 ternary system. Experimental results (d_{220} in italics) with 2σ error bars. Selected results have been plotted for clarity. (**B**) Same data recalculated for log P_{O_2} in the 1300 °C isothermal section. Broken lines show Fe^{3+} content of magnesiowüstite ($\alpha \times 100\%$). The set of 2 standard error bars shown are representative for the whole diagram.

of Equilibrium 2 is close to that of the Fe-FeO and Ni-NiO buffers.

At higher *P*, phase changes in the more-oxidized spinel phases (Mao and Bell 1975; Mao et al. 1977) significantly reduce Fe^{3+} solubility in magnesiowüstite (e.g., McCammon et al. 1995; Stølen and Gronvøld 1996). Mao and co-workers bracketed the reaction in magnesioferrite to 160 ± 40 kbar at 1500 °C, and McCammon found reduced Fe^{3+} solubility in magnesiowüstites at 180 kbar and 1000 °C. Our experiments at 150 kbar and 1300 °C show reduced solubility. This renders the use of Fe^{3+} in magnesiowüstite inappropriate as an oxybarometer above 150 kbar.

ACKNOWLEDGMENTS

The Mössbauer data presented here were collected under the auspices of the University of London Intercollegiate Research Service. The authors thank I. Wood for his assistance in XRD experiments. This research was funded from NERC grant GR310330. J.B. is grateful for his Royal Society University Research Fellowship.

REFERENCES CITED

Biggar, G.M. (1974) Oxygen partial pressures; control, variation, and measurement in quench furnaces at one atmosphere total pressure. Mineralogical Magazine, 39, 580–586.

Brynstead, J. and Flood, H. (1958) The redox equilibrium in solid solutions of wüstite and magnesium oxide. Zeitschrift für Elektrochimie, 62, 953–958.

Dobson, D.P., Richmond, N.C., and Brodholt, J.P. (1997) A high temperature electrical conduction mechanism in the lower mantle phase $(Mg,Fe)_{1-x}O$. Science, 275, 1779–1781.

Gourdin, W.H., Kingery, W.D., and Driear, J. (1979) The defect structure of MgO containing trivalent cation solutes: the oxidation-reduction behaviour of iron. Journal of Materials Science, 14, 2074–2082.

Hazen, R.M. and Jeanloz, R. (1984) Wüstite ($Fe_{1-x}O$): a review of its defect structure and physical properties. Reviews of Geophysics and Space Physics, 22, 37–46.

Long, G.J. and Grandjean, F. (1991) Mössbauer effect, magnetic and structural studies of wüstite, $Fe_{1-x}O$. Advances in Solid-State Chemistry, 2, 187–221.

McCammon, C.A., Harris, J.W., Harte, B., and Hutchison, M.T. (1995) Ferric iron content of (Fe,Mg)O from lower mantle diamond inclusions. In D.L. Anderson, S.R. Hart, and A.W. Hofmann, conveners, Plume 2, Terra Nostra, 3, p 91–94. Alfred-Wegener-Stiftung, Bonn.

Mao, H.K. and Bell, P.M. (1975) High pressure transformation in magnesioferrite ($MgFe_2O_4$). Annual Report of the Director of the Geophysical Laboratory Year Book, 74, 555–557.

Mao, H.K., Virgo, D., and, Bell, P.M. (1977) High-pressure ^{57}Fe Mössbauer data on the phase and magnetic transitions of magnesioferrite ($MgFe_2O_4$), magnetite (Fe_3O_4), and hematite (Fe_2O_3). Annual Report of the Director of the Geophysical Laboratory Year Book, 76, 522–525.

Speidel, D.H. (1967) Phase equilibria in the system MgO-FeO-Fe_2O_3: The 1300 °C isothermal section and extrapolations to other temperatures. Journal of the American Ceramics Society, 50, 243–248.

Stølen, S. and Gronvøld, F. (1996) Calculation of the phase boundaries of wüstite at high pressure. Journal of Geophysical Research, 101, 11531–11540.

Taylor, W.R. and Green, D. (1988) The role of C-O-H fluids in mantle partial melting. In J. Ross, A. Jaques, J. Ferguson, D. Green, S. O'Rielly, R. Dauchin, and A. Jouse, Eds., Kimberlites and related rocks, Vol. 1, p. 592–602. Geological Society of Australia, Sydney.

Valet, P-M., Pluschkell, W., and Engell, H-J. (1975) Equilibria between MgO-FeO-Fe_2O_3 solid solutions and oxygen. Archive Eisenhüttenwes, 46, 383–388.

Wood, B.J. and Nell, J. (1991) High temperature electrical conductivity of the lower mantle phase (Mg,Fe)O. Nature, 351, 309–311.

MANUSCRIPT RECEIVED JULY 31, 1997
MANUSCRIPT ACCEPTED FEBRUARY 21, 1998
PAPER HANDLED BY ROBERT W. LUTH